

Electron transport in high-entropy alloys: $\text{Al}_x\text{CrFeCoNi}$ as a case study.

J. Kudrnovský,* V. Drchal, and F. Mácá

Institute of Physics ASCR, Na Slovance 2, CZ-182 21 Praha 8, Czech Republic

I. Turek

Institute of Physics of Materials ASCR, Žitkova 22, CZ-616 62 Brno, Czech Republic

S. Khmelevskiy

*Center for Computational Materials Science, Institute for Applied Physics,
Vienna University of Technology, Wiedner Hauptstrasse 8, A-1040 Vienna, Austria*

(Dated: July 24, 2019)

The high-entropy alloys $\text{Al}_x\text{CrFeCoNi}$ exist over a broad range of Al concentrations ($0 < x < 2$). With increasing Al content their structure is changed from the fcc to bcc phase. We investigate the effect of such structural changes on transport properties including the residual resistivity and the anomalous Hall resistivity. We have performed a detailed comparison of the first-principles simulations with available experimental data. We show that the calculated residual resistivities for all studied alloy compositions are in a fair agreement with available experimental data as concerns both the resistivity values and concentration trends. We emphasize that a good agreement with experiment was obtained also for the anomalous Hall resistivity. We have completed study by estimation of the anisotropic magnetoresistance, spin-disorder resistivity, and Gilbert damping. The obtained results prove that the main scattering mechanism is due to the intrinsic chemical disorder whereas the effect of spin polarization on the residual resistivity is appreciably weaker.

I. INTRODUCTION

The high-entropy alloys (HEA), the multicomponent crystalline alloys, often also called multi-principal element alloys have attracted a quite significant and growing interest in the last decade. Of the vast existing literature we just mention a recent book,¹ a critical review,² and an overview of possible theoretical approaches.³ The high entropy of mixing of these multicomponent alloys suppresses the formation of ordered intermetallic compounds leading to well disordered phases with simple lattice structures such as the face-centered cubic (fcc) or the body-centered cubic (bcc) ones. Magnetic HEA's that consist of magnetic 3d-elements are particularly interesting. A typical example is the so-called quinary Cantor alloy (CrMnFeCoNi) consisting of equiconcentration disordered mixture of magnetic Cr, Mn, Fe, Co, and Ni elements with an fcc structure. Such alloy offers a richness of magnetic properties depending on the sample preparation.⁴ The structural change from the fcc to bcc phase was predicted by *ab initio* molecular dynamics simulations⁵ for Cantor-like alloys with Cr substituted by another metallic element with formula CoFeMnNiX ($X = \text{Al, Ga, and Sn}$).

By doping with *sp*-elements, which influences carrier concentration in the conduction band and thus both the magnetic and transport properties, and even the alloy structure one can search for new functional properties. A typical example of such alloy is $\text{Al}_x\text{CrFeCoNi}$ alloy^{6,7} with x ranging from $x=0$ to $x=2$. In particular, alloying with increasing Al content stabilizes the bcc phase from the original fcc phase of quaternary CrFeCoNi alloy. Another interesting property, also present in the

Cantor alloy, is a large residual resistivity of the order of $100 \mu\Omega\text{cm}$ which is in a striking contrast to a much smaller resistivity of the binary fcc NiFe or fcc NiCo counterparts. The large values of the residual resistivity in HEA's are caused by strong scattering on the intrinsic chemical disorder. In the present work we apply the alloy-specific first-principles methodology based on the Kubo-Greenwood formula⁸ which was successfully used for binary alloys^{9,10} also to HEA's in order to estimate the intrinsic contribution to the resistivity and compare them to available experimental data.

Contrary to the experimental and theoretical studies of structural and thermodynamical properties of HEA's the studies of electronic transport are very rare.² The transport properties, together with the electronic structure are among the most important material properties. The theoretical tools for the resistivity study are more complicated and not so broadly available as electronic structure codes focused on total energies, electron densities and magnetic moments. Recently, theoretical transport studies of the Cantor fcc CrMnFeCoNi alloy¹¹ and of a related medium-entropy fcc NiCoMn alloy¹² appeared which studied various possible scattering mechanisms contributing to the residual resistivity. However, theoretical investigation of the effect of Al-doping on the resistivity, as well as of the role of different structures (bcc, fcc) for electron transport in AlCrFeCoNi, is still missing. Moreover, in addition to residual resistivities also the anomalous Hall resistivity (AHR) for both structure phases was determined experimentally.^{6,7} Therefore, these alloys are an obvious choice for *ab initio* based studies of transport properties in HEA's containing *sp*-elements. In the present study, also the anisotropic mag-

netoresistance (AMR), the spin-disorder resistivity and the Gilbert damping for both structures and typical Al concentrations are calculated and discussed.

II. FORMALISM

The disordered fcc and bcc phases of $\text{Al}_x\text{CrFeCoNi}$ alloy with x ranging from $x=0$ to $x=2$ were studied for experimentally observed phases and lattice constants.⁶ The fcc phase exists roughly for $x < 0.5$ while the bcc phase is stable for $x > 1.0$, but boundaries are not well defined. Duplex phase (a mixture of fcc and bcc phases) exists for the intermediate Al concentrations. We note that sometimes the $\text{Al}_x\text{CrFeCoNi}$ alloy is presented as $\text{Al}_{1-4y}\text{Cr}_y\text{Fe}_y\text{Co}_y\text{Ni}_y$, where $y = 1/(4+x)$ and the sum of all component concentrations is one.²

The spin-polarized electronic structure calculations were done using the Green function formulation of the tight-binding linear muffin-tin orbital (TB-LMTO) method in the atomic sphere approximation (ASA).¹³ We employ the scalar-relativistic version of the TB-LMTO method and, in order to assess the importance of the relativistic effects, we also made calculations using the fully relativistic version of the TB-LMTO method. In both cases the exchange-correlation potential of Vosko, Wilk and Nusair (VWN)¹⁴ and the *spd*-basis set were used. The alloy disorder in studied multicomponent alloys is described in the framework of the coherent potential approximation (CPA).¹⁵ The use of the CPA allows us to work very efficiently in small fcc or bcc unit cells. On the contrary, large special-quasirandom structure (SQS) supercells are needed in conventional density-functional-theory (DFT) studies.^{4,5} It should be noted that continuously varying Al content imposes additional non-trivial constraints on the choice of a suitable SQS-supercell. The cost we pay for using the CPA is the neglect of possible local environment and clustering effects in the alloy which, on the other hand, are captured by the SQS-supercell approach. The CPA is a reliable approach in well disordered alloys, particularly when the concentration trends are concerned. Even more important advantage of the CPA is the fact that it provides naturally transport relaxation times which need not be taken from outside like, e.g., in the Boltzmann equation approach.

The transport properties are described by the conductivity tensor σ with components $\sigma_{\mu\nu}$ ($\mu, \nu=x, y, z$). The resistivity tensor ρ with components $\rho_{\mu\nu}$ is obtained simply by inversion of the conductivity tensor, $\rho = \sigma^{-1}$. The conductivity tensor is determined in the framework of the Kubo-Greenwood (K-G) approach (only diagonal elements of $\sigma_{\mu\nu}$ are non-zero in present cubic systems in the scalar-relativistic model).⁸ The off-diagonal components of $\sigma_{\mu\nu}$ are needed for the AMR/AHR studies and they are calculated in the framework of the Kubo-Bastin (K-B) formulation of the fully-relativistic transport in disordered magnetic alloys which includes both the Fermi-surface and Fermi-sea terms on equal footing.⁹

The Fermi-surface term contains contribution only from the states at the Fermi energy and includes the most important elastic scattering effects due to impurities. The Fermi-sea term, on the contrary, depends on all occupied states below the Fermi energy; this term contributes only to the antisymmetric part of the tensor $\sigma_{\mu\nu}$. Once the transport tensor is determined, the AHR= ρ_{xy} while the AMR= $(\rho_{zz} - \rho_{xx})/\rho_{\text{tot}}$, where ρ_{tot} is the average value of diagonal components of the resistivity tensor. In relativistic calculations we assume that the magnetic moment points in the z-direction. The disorder-induced vertex corrections,¹⁰ which describe the correlated motion of two electrons in a random alloy potential, are included. They correspond to the backward scattering contribution in the conventional Boltzmann equation approach.

The Gilbert damping (GD) constant is an important phenomenological parameter describing the magnetization dynamics. It is evaluated here with the help of a recently developed approach using nonlocal torques¹⁶ as an alternative to the usual local torque operators entering the torque-correlation formula.¹⁷⁻¹⁹ This leads to effective torques that are represented as non-site-diagonal and spin-independent matrices, which simplifies evaluation of disorder-induced vertex corrections which play essential role in the present formulation since their neglect would lead to quantitatively and physically incorrect results.¹⁶

Our formulation gives results that compare well to other first-principles studies.¹⁷⁻¹⁹ In this study we will concentrate on the GD due to chemical disorder, especially the effect of Al-doping. It should be noted that there are other sources of damping, e.g., the temperature effects due to phonons and spin fluctuations which are neglected here.

III. RESULTS

A. Electronic structure and magnetic moments

The results of electronic structure calculations serve as an input for transport calculations of $\text{Al}_x\text{CrFeCoNi}$ alloys.

To illustrate the underlying electronic structure, we show in Figs. 1 and 2 the total and component-resolved densities of states (DOS) for two typical alloys, namely, fcc $\text{Al}_{0.25}\text{CrFeCoNi}$ and bcc $\text{Al}_{1.25}\text{CrFeCoNi}$. The following conclusions can be done: (i) We note a typical two-peak-like total DOS characteristic of the bcc phase as compared to an essentially one-peak-like total DOS for the fcc phase. In both cases the Fermi level is located deep inside the valence band as it is typical for metallic systems in contrast, e.g., to doped semiconductors in which the clustering has a non-negligible effect on DOS close to band edges. The CPA is thus a good approximation for electron transport studies; (ii) We also note larger total DOS at the Fermi energy for fcc phase as compared to the bcc phase. This indicates a larger amount of carriers and thus a smaller resistivity/larger conductivity

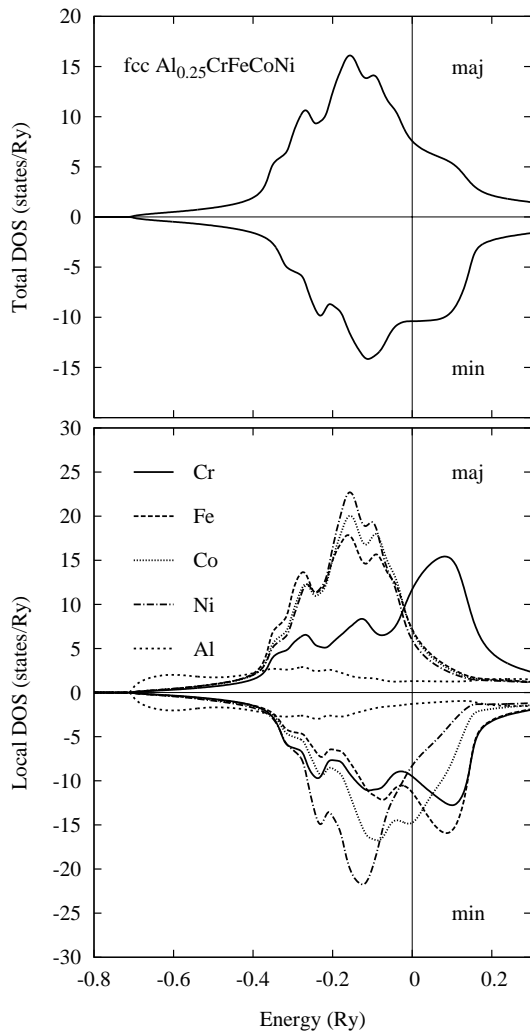


FIG. 1: Calculated spin-resolved DOS's for fcc $\text{Al}_{0.25}\text{CrFeCoNi}$ alloy: the total DOS (upper frame) and atom-resolved DOS's (lower frame) are shown. The vertical lines denote the position of the Fermi level.

of fcc phases because the amount of disorder is similar in both phases (see atom-resolved DOS's below and discussion there); (iii) The Al-resolved DOS is free-electron like with only small modifications in the energy region where it hybridizes with transition metal states; (iv) The majority Ni-, Co-, and Fe-resolved DOS's indicate only negligible influence of the disorder: they all have similar shapes and centers of gravity and resemble corresponding total DOS. On the contrary, the majority Cr-DOS has the center of gravity shifted to higher energies and its shape is different from those of Ni-, Co-, and Fe-states. This is due to a lower atomic number of Cr and thus a weaker Coulomb attraction in comparison with Fe, Co, and Ni. Majority Cr states thus introduce a significant disorder in the majority band. Below we show that in present alloys the resistivity in both majority and minority channels is comparable (see also Ref.20); (v) The minority Ni-,

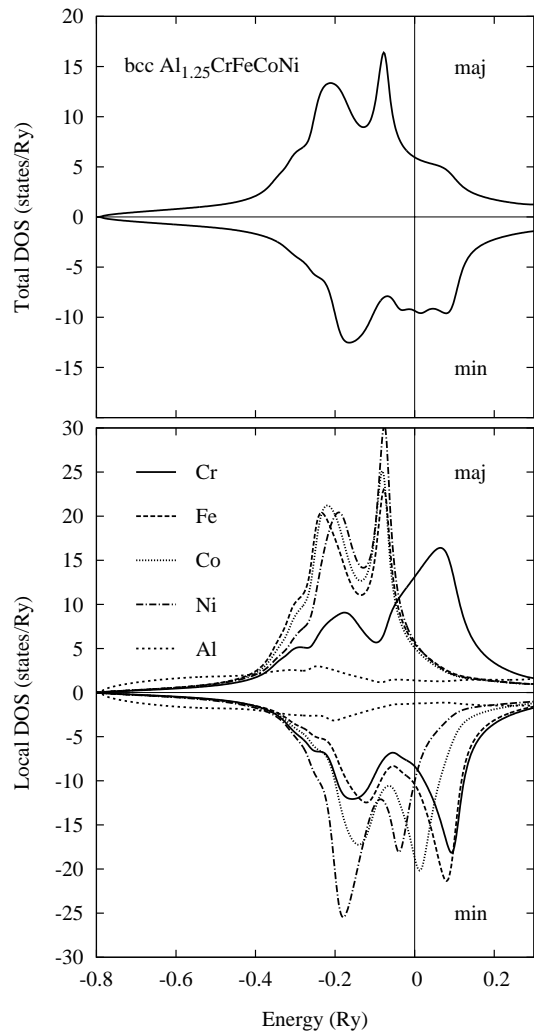


FIG. 2: The same as in Fig. 1 but for bcc $\text{Al}_{1.25}\text{CrFeCoNi}$ alloy.

Co-, Fe-, and Cr-resolved DOS's have centers of gravity shifted to different positions thus indicating the presence of disorder among all components as contrasted to the majority states. It should be noted that the character of disorder in both fcc and bcc phases is quite similar. The presence of non-negligible disorder in both majority and minority states is the reason of much larger resistivity of $\text{Al}_x\text{CrFeCoNi}$ alloys as compared to the Ni-rich NiFe and NiCo alloys in which the disorder effect in majority spin channel is negligible.²⁰ The disorder effect is essential for both, minority and majority spin channels, but operates in them differently. This observation provides us with a motivation to study the magnetotransport phenomena.

We present magnetic properties in Table 1, where we show the total and local magnetic moments for alloys with $x = 0.25$ and $x = 1.25$. We can make the following conclusions: (i) The induced local Al moments are very small and negative. Also moments on Cr atoms are negative and their absolute value is reduced with in-

TABLE I: Calculated total magnetic moment (M_{tot}) and local magnetic moments (m^X , X=Al, Cr, Fe, Co, Ni) for $\text{Al}_x\text{CrFeCoNi}$ alloys in the fcc ($x_{\text{Al}} = 0.25$) and bcc ($x_{\text{Al}} = 1.25$) phases. Magnetic moments are in μ_{B} .

x_{Al}	M_{tot}	m^{Al}	m^{Cr}	m^{Fe}	m^{Co}	m^{Ni}
0.25 (fcc)	0.606	-0.054	-0.620	1.933	1.027	0.253
1.25 (bcc)	0.646	-0.045	-0.103	2.117	1.243	0.191

creasing Al content. The present alloys are thus ferromagnets. The values of Ni-local moments are strongly reduced as compared to the fcc Ni crystal; (ii) Dominating moments are those on Co and, first of all, on Fe sites which have values close to the values in bcc Fe crystal while moments on Co-sites are smaller as compared to fcc-Co crystal. Both moments depend weakly on the Al doping; and (iii) Due to the character of local moments, both alloys have non-zero total magnetization with total moments slightly larger for the bcc phase and relatively small in their sizes, being of order $0.5 \mu_{\text{B}}$. We note a good quantitative agreement of present moments with a recent theoretical study.²¹

The present CPA calculations ignored any spin fluctuations in the ground state of the alloys. However, existing studies of the Cantor CrMnFeCoNi alloy¹¹ and of the ternary fcc NiCoMn system¹² revealed an instability of Mn atoms to form more complicated moment distributions; we have verified this feature for the quinary Cantor alloy by using the well-known CPA approach.²² In order to examine a similar instability of Cr atoms in the present $\text{Al}_x\text{CrFeCoNi}$ systems, we have performed the CPA calculations which started with multiple Cr magnetic moments. For both structures (fcc and bcc), the iterations converged always to the same single value of Cr moment. This indicates that the present AlCrFeCoNi systems can be reasonably described by assuming the same (average) local moment attached to each alloy species.

B. Residual resistivities

The theoretical estimate of residual resistivity ρ_0 and its comparison with available experiments^{6,7,23} is the main result of the present paper. We treat the fcc and bcc phases as disordered alloys described by the CPA. Corresponding electronic structure provides also naturally the transport relaxation times as used in the K-G formula for estimate of resistivities. We note that the SQS-supercell calculations (see, e.g., Refs.4,5) indicate the presence of local environment effects, both in atomic structure and spins, which are neglected here. On the other hand, local environment effects appear as fluctuations around average atomic levels. Although such fluctuations are large in some cases, they usually correspond to states with small weights. One can thus say that the intrinsic chemical disorder due to many atomic components will dominate. Considering further the fact that the CPA gives reliably

concentration trends, we can conclude that present approach represents reasonable first approximation to estimate resistivities in the present HEA's.

Results are shown in Fig. 3 for both fcc and bcc $\text{Al}_x\text{CrFeCoNi}$ alloys for which experiments^{6,7} are available.

Let us start with experiment Ref.6 (see also Ref.23). It should be noted that experiment was done at the room temperature while calculations relate to $T = 0$ K. We note an enhancement of the resistivity due to the lattice vibrations and spin fluctuations induced by a finite temperature. It is possible to include, for simple systems, the effect of temperature in the framework of the alloy analogy model as formulated in the CPA.²⁴ It should be noted that although a success was recently reached by a modified approach for fcc alloys with few alloy constituents²⁵ such a detailed study of temperature effects is beyond the scope of the present paper. Under such situation we decided just to scale the zero temperature results by an empirical constant to account for the finite temperature effects. We have chosen this factor to be 1.2 motivated by the experiment⁷ in which resistivity ratio for 300 K to 0 K was measured for many samples of different compositions. The purpose is just to see the effect of the finite temperature. Results are shown in Figs. 3a,3b. Already large values of ρ_0 exist for $x_{\text{Al}} = 0.0$, i.e., for the equiconcentration quaternary CrFeCoNi alloy, which agrees very well with a recent theoretical study.¹¹ We observe an increase of ρ_0 with increasing Al content in both the fcc and bcc phases. This result as well as large values of ρ_0 are due to the fact that d -states of Al are missing and thus Al has a low density of states around the Fermi energy in comparison with other alloy components introducing thus a strong scattering. For example, in disordered bcc $\text{Fe}_{1-x}\text{Al}_x$ alloys²⁶ the experimental ρ_0 is about $150 \mu\Omega\text{cm}$ at $T=4$ K for x_{Al} around 0.3. Similarly, the random bcc $\text{V}_{0.75}\text{Al}_{0.25}$ alloy exhibits practically the same resistivity.²⁷ Comparable values are obtained for $\text{Al}_x\text{CrFeCoNi}$ for large x_{Al} in the bcc phase.

There is a good quantitative agreement of calculated and measured ρ_0 in both fcc and bcc regions, in particular for the scaled model. In agreement with the experiment the slope of the concentration dependence of ρ_0 is larger for the fcc phase as compared to the bcc one, although the effect is more pronounced in the experiment.

It is a well-known fact²⁰ that a significant increase of the resistivity occurs in Ni-rich NiFe and NiCo fcc alloys due to the mixing of spin-channels by the spin-orbit coupling. We have therefore performed also fully-relativistic calculations for $x_{\text{Al}} = 0.25$ and $x_{\text{Al}} = 1.25$ alloys with fcc and bcc phases, respectively. We have obtained only a small changes of ρ_0 , namely, ρ_0 was $86.16 \mu\Omega\text{cm}$ vs $84.70 \mu\Omega\text{cm}$ for $x_{\text{Al}} = 0.25$, and $137.42 \mu\Omega\text{cm}$ vs $135.03 \mu\Omega\text{cm}$ for $x_{\text{Al}} = 1.25$. In both cases, higher values correspond to the fully-relativistic model. The origin of large enhancement of ρ_0 by spin-orbit coupling in the above-mentioned binary alloys is the existence of disorder-free majority bands, which are missing here.

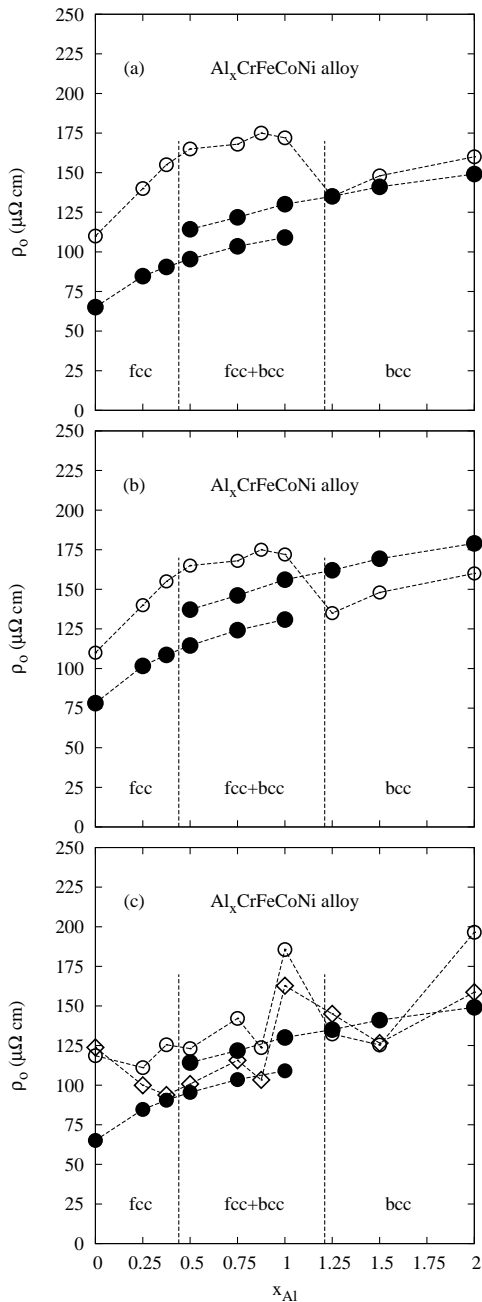


FIG. 3: Calculated and experimental residual resistivities ρ_0 as a function of Al concentration x_{Al} . Dashed vertical lines denote approximate boundaries between the fcc, duplex, and bcc phases. Note that the fcc phase extends into duplex phase (fcc + bcc) and similarly the bcc phase starts in duplex phase. Filled circles denote theoretical results while empty symbols correspond to experimental data. (a) Experiment Ref.6 at room temperature compared with theoretical results for $T = 0$ K. (b) The same as (a) but theoretical results are scaled by a factor 1.2 to fit experiment done at room temperature (see text). (c) Comparison of experiment, Ref.7, with theoretical results. Empty circles and empty boxes denote alloys 'as-cast' and 'homogenized', respectively (see experimental paper for details). Both the theory and experiment now correspond to $T = 0$ K.

The contributions of the spin-up (σ^\uparrow) and spin-down (σ^\downarrow) conductivity channels to the total conductivity are comparable. For example, σ^\uparrow (σ^\downarrow) = 4.77 (7.04) kS/cm for $x_{Al} = 0.25$, and σ^\uparrow (σ^\downarrow) = 3.85 (3.56) kS/cm for $x_{Al} = 1.25$, respectively. We can thus conclude that relativistic effects are small in the studied alloy.

Theoretical description of the duplex region in which both phases co-exist is difficult because of the lack of structural details. We therefore present separately results for the fcc phase with Al concentrations extending into the duplex (fcc+bcc) region, and similarly, we start the bcc phase in the duplex region. Corresponding lattice constants were taken from Ref.6. We have thus avoided any processing of results like, e.g., the serial or parallel resistivities, the arithmetic weighting, etc. Inhomogeneity of samples in the duplex region is obvious.

Recently Singh et al.²⁸ have shown on the basis of calculations of chemical interatomic interactions that considered $Al_xCrFeCoNi$ alloys can exhibit a tendency to the clustering in the fcc phase while in the bcc phase can exist ordering tendency. One can thus speculate that this can be one of possible reasons for the smaller/larger calculated resistivities for fcc/bcc phases as compared to the experimental ones .

Next we will discuss the experiment of Ref.7. Results are presented in Fig. 3c with the following comments: (i) Contrary to the experiment⁶ there is no clear concentration trend. Fluctuating values of ρ_0 may indicate sample inhomogeneity due to its preparation. Largest fluctuations are, as expected, in the duplex region. Larger fluctuations are also for 'as-cast' samples as compared to 'homogenized' ones; and (ii) Nevertheless, calculated and measured resistivity values are still in acceptable agreement, as well as larger resistivities for higher x_{Al} (bcc phase). Experiment gives no detailed structural data concerning studied samples, just its Al-content so that more detailed discussion of measured resistivity fluctuations and their comparison with the experiment is not possible.

We note that the performed calculations of residual resistivity ignore the effect of local atomic relaxations, which provide an additional mechanism of electron scattering. Since we cannot determine the magnitude of the local relaxations quantitatively, we have performed only a preliminary study in order to get rough estimation of their effect on the resistivity by employing the alloy analogy model in the CPA.^{24,29} As a typical mean value of the atomic displacement, we took $\Delta u = 0.05$ Å for fcc alloys (obtained for the fcc Cantor alloy)¹¹ and a slightly higher value $\Delta u = 0.075$ Å for bcc alloys (because of the more open bcc geometry). The resulting increase of the residual resistivity of $Al_xCrFeCoNi$ was small in both structures, being about 2.8 % for $x = 0.25$ in the fcc case and about 1.4 % for $x = 1.25$ in the bcc case. These results agree qualitatively with those of Ref.11 proving the dominating effect of strong intrinsic chemical disorder on the resistivity. A more systematic study of the role of local atomic relaxations goes beyond the scope of

the present work.

One can summarize that the CPA, despite of its simplicity, is able to reproduce the main features of measured resistivities also in such complex alloys like $\text{Al}_x\text{CrFeCoNi}$. Clearly, the main reason for this success is the dominance of intrinsic chemical disorder in alloy. On the other hand, one should keep in mind that calculated values are influenced by the neglect of lattice relaxations. In general, one could say that lattice relaxations roughly represent site-off diagonal disorder which have much smaller effect as compared to the dominating chemical disorder related to different positions of atomic alloy levels.

C. Spin-disorder resistivity (SDR)

The SDR is the resistivity caused by spin fluctuations that exist at finite temperature in the paramagnetic state above the Curie temperature. The local moments still exist but they are oriented randomly in such a way that the total magnetic moment is zero. From the theoretical point of view the SDR can be simulated successfully in the framework of the CPA as the resistivity of an equiconcentration alloy of spin moments pointing in opposite directions (the disordered local moment (DLM) state).³⁰ The fluctuating local moments are then determined selfconsistently in the framework of the DFT. In the fcc region only local moments on Fe-sites are nonzero, all other collapse to zero. In the bcc region, in addition, local moments on Co atoms survive. Such result, in general, is not correct as, e.g., the local DLM moment in fcc Ni collapses to zero but the experiment indicates its nonzero value at the Curie temperature. These values can be found theoretically not only for fcc Ni,³¹ but also for binary alloys.³² The situation is much more complicated for the present multicomponent alloy. We therefore determine just the lower and upper limits of the SDR. The lower limit is the above DLM result, the upper limit corresponds to the DLM state which is constructed on the basis of an FM solution assuming the frozen Fermi energy and frozen potential parameters.³¹ It is denoted as $\rho_{\text{max}}^{\text{SDR}}$.

TABLE II: The spin disorder resistivity (SDR, the resistivity due to spin fluctuations in the paramagnetic state) of $\text{Al}_x\text{CrFeCoNi}$ for two values of Al concentrations, namely, $x_{\text{Al}} = 0.25$ (fcc) and $x_{\text{Al}} = 1.25$ (bcc) are shown. We present the SDR results for two models, one in which the SDR is identified with the resistivity of the DLM state ($\rho_{\text{DLM}}^{\text{SDR}}$) and the other ($\rho_{\text{max}}^{\text{SDR}}$) in which the DLM state is constructed from the corresponding FM solutions with frozen Fermi energies and frozen potential parameters. For a comparison we also show conventional resistivities (ρ_{FM} , see Fig. 3) and resistivities of non-magnetic phases (ρ_{NM}). All values are in $\mu\Omega\text{cm}$.

x_{Al}	ρ_{FM}	ρ_{NM}	$\rho_{\text{DLM}}^{\text{SDR}}$	$\rho_{\text{max}}^{\text{SDR}}$
0.25 (fcc)	84.70	72.16	83.98	89.97
1.25 (bcc)	135.03	117.17	132.17	137.49

Results for two Al concentrations are summarized in Table 2 in which we have added for a comparison also resistivities of the reference FM state and resistivities of corresponding non-magnetic phases. We have following comments: (i) The non-magnetic phases have slightly smaller resistivities as compared not only to the DLM phases but also as compared to the reference FM phase. The effect of magnetic scatterings is thus less relevant than the effect of different atom types and their different potentials; (ii) Slightly larger values of the reference ρ_{FM} as compared to $\rho_{\text{DLM}}^{\text{SDR}}$ are due to the fact that in the DLM state in the fcc/bcc phase are non-zero only Fe and perhaps also Co moments. Missing magnetic scattering thus leads to smaller resistivities (see also discussion in (i)); and (iii) On the contrary, the $\rho_{\text{max}}^{\text{SDR}}$ is slightly larger due to the presence of fluctuating moments on Cr, Fe, Co, and Ni atoms. One can thus conclude that due to already large resistivity of the reference FM state, the spin disorder influences resistivity only weakly.

D. Anisotropic magnetoresistance, anomalous Hall resistivity, and Gilbert damping

We calculate further quantities which are due to the spin-orbit coupling, namely, the AMR and the AHR for two typical Al-concentrations, namely, $x_{\text{Al}} = 0.25$ (fcc phase) and $x_{\text{Al}} = 1.25$ (bcc phase). The relativistic input is needed to solve the K-B transport equation.⁹ While we have found no experimental data for the AMR, the AHR data are available for the above two alloys.⁶

TABLE III: Calculated AMR and AHR for $\text{Al}_x\text{CrFeCoNi}$ alloys in the fcc ($x_{\text{Al}} = 0.25$) and bcc ($x_{\text{Al}} = 1.25$) phases. The AMR values are in % while the AHR values are in $\mu\Omega\text{cm}$.

x_{Al}	AMR	AHR _{th}	AHR _{exp}
0.25 (fcc)	0.031	0.879	0.5
1.25 (bcc)	0.044	1.699	1.5

Calculated results are summarized in Table 3 with the following conclusions: (i) The AMR is positive, but its values are very small, considering the fact that, e.g., for Ni-rich NiFe the AMR can be as large as 15%.^{20,33} It was shown that large values of the AMR in fcc Ni-rich alloys are due to essentially disorder-free majority bands. On the contrary, the Ni-rich NiMn alloy has disorder in both the majority and minority bands and significantly lower AMR than Ni-rich NiFe, but still few times larger than the present alloys. In addition to very similar disorder in both channels in present alloys, the other reason of such small AMR can be the ferrimagnetic rather than the FM character of present alloys with the antiparallel Cr moments. Its role plays also small total moment of studied HEA alloys; and (ii) There is a good agreement between calculated and measured AHR for the bcc phase ($x_{\text{Al}} = 1.25$) while the agreement for the fcc phase ($x_{\text{Al}} = 0.25$) is worse but still reasonable. We note that a good

agreement of both calculated resistivities and AHR with experiment is a non-trivial result.

We have estimated GD parameters for the same typical concentrations as above for the AHR. Calculated values of the GD parameter for fcc ($x_{\text{Al}} = 0.25$) and bcc ($x_{\text{Al}} = 1.25$) phases are, respectively, 0.00655 and 0.00585. Both values are similar which is compatible with similar values of the DOS at the Fermi level and the total magnetization whose ratio is a rough estimate of the GD parameter, which explains also rather large values due to small total spin moments in both alloys. Calculated values of GD parameter are comparable to those in Ni-rich fcc NiFe alloy but are larger as compared to bcc-FeCo alloy.¹⁶

IV. CONCLUSIONS

Transport properties of the fcc and bcc phases of the high-entropy $\text{Al}_x\text{CrFeCoNi}$ alloys were calculated over a broad range of Al concentrations using the DFT-based simulations. The main conclusions from numerical studies can be summarized as follows: (i) The agreement of calculated residual resistivities with available experimental data is good for both fcc and bcc phase. In particular, the resistivity values as well as larger resistivity of the bcc-phase as compared to the fcc one agree with both experiments. Calculation even reproduce details of concentration trends in one of the experiment.⁶ (ii) The major contribution to the residual resistivity is due to the intrinsic chemical disorder while the magnetic

disorder has smaller effect. The increase of ρ_0 with increasing Al concentration in both fcc and bcc phases and its large values in particular in the latter one are due to strong scatterings on Al atoms; (iii) The calculated values of anisotropic magnetoresistance are positive but very small being less than 0.05% for both fcc and bcc phases; (iv) The spin disorder influences resistivity only weakly because of already large resistivity of the reference FM state; (v) Estimated values of the Gilbert damping are comparable for chosen typical fcc and bcc phases and are rather large (of order 0.006) due to small total spin moments; and (vi) The estimated anomalous Hall resistivity again agrees well for the bcc phase while agreement with the experiment for the fcc phase is worse though still acceptable.

The present results thus suggest that the CPA captures the main scattering mechanism due to intrinsic alloy disorder and gives acceptable description even for such complex alloys like the studied one.

Acknowledgments

The work of J.K., V.D, F.M., and I.T. was supported by a Grant from the Czech Science Foundation (No. 18-07172S) and S.K. thanks for support from the Center for Computational Materials Science, Vienna University of Technology. We acknowledge the support from the National Grid Infrastructure MetaCentrum (project CES-NET LM2015042) and the Ministry of Education, Youth and Sports (project LM2015070).

* Electronic address: kudrnov@fzu.cz

¹ M. C. Gao, J.-W. Yeh, P. K. Liaw, Y. Zhang (Eds.), *High-entropy Alloys: Fundamentals and Applications*, Springer, New York, 2016.

² D. B. Miracle, O. N. Senkov, A critical review of high-entropy alloys and related concepts, *Acta Mater.* **122**, 448-511 (2017).

³ S. Mu, Z. Pei, X. Liu, G. M. Stocks, Electronic transport and phonon properties of maximally disordered alloys: From binaries to high-entropy alloys, *J. Mater. Res.* **33**, 2857-2880 (2018).

⁴ O. Schneeweiss, M. Friák, M. Dudová, D. Holec, M. Šob, D. Kriegner, V. Holý, P. Beran, E. P. George, J. Neugebauer, A. Dlouhý, Magnetic properties of the CrMnFeCoNi high-entropy alloy, *Phys. Rev. B* **96**, 014437 (2017).

⁵ T. Zuo, M. C. Gao, L. Ouyang, X. Yang, Y. Cheng, R. Feng, S. Chen, P. K. Liaw, J. A. Hawk, Y. Zhan, Tailoring magnetic behavior of CoFeMnNiX (X = Al, Cr, Ga, and Sn) high-entropy alloys by metal doping, *Acta Mater.* **130**, 10-18 (2017).

⁶ H.-P. Chou, Y.-S. Chang, S.-K. Chen, J.-W. Yeh, Microstructure, thermophysical and electrical properties in $\text{Al}_x\text{CoCrFeNi}$ ($0 \leq x \leq 2$) high-entropy alloys, *Mater. Sci. Eng. B* **163**, 184-189 (2009).

⁷ Y.-F. Kao, S.-K. Chen, T.-J. Chen, P.-C. Chu, J.-W. Yeh, S.-J. Lin, Electrical, magnetic, and Hall properties of $\text{Al}_x\text{CoCrFeNi}$ high-entropy alloys, *J. Alloys Compd.* **509**,

1607 (2011).

⁸ I. Turek, J. Kudrnovský, V. Drchal, L. Szunyogh, and P. Weinberger, Interatomic electron transport by semiempirical and ab initio tight-binding approaches, *Phys. Rev. B* **65**, 125101 (2002).

⁹ I. Turek, J. Kudrnovský, and V. Drchal, Fermi sea term in the relativistic linear muffin-tin-orbital transport theory for random alloys, *Phys. Rev. B* **89**, 064405 (2014).

¹⁰ K. Carva, I. Turek, J. Kudrnovský, and O. Bengone, Disordered magnetic multilayers: Electron transport within the coherent potential approximation, *Phys. Rev. B* **73**, 144421 (2006).

¹¹ S. Mu, G. D. Samolyuk, S. Wimmer, M. C. Tropicovsky, S. Khan, S. Mankovsky, H. Ebert, G. M. Stocks, Uncovering electron scattering mechanisms in NiFeCoCrMn derived concentrated solid solutions and high entropy alloys, *npj Comput. Materials* **5**, 1 (2019).

¹² Sai Mu, J. Yin, G. D. Samolyuk, S. Wimmer, Z. Pei, M. Eisenbach, S. Mankovsky, H. Ebert, and G. M. Stocks, Hidden Mn magnetic-moment disorder and its influence on the physical properties of medium-entropy NiCoMn solid solution alloys, *Phys. Rev. Mater.* **3**, 014411 (2019).

¹³ I. Turek, V. Drchal, J. Kudrnovský, M. Šob, and P. Weinberger, *Electronic structure of disordered alloys, surfaces and interfaces*, Kluwer, Boston-London-Dordrecht, 1997.

¹⁴ S. H. Vosko, L. Wilk, and M. Nusair, Accurate spin-dependent electron liquid correlation energies for local spin

- density calculations: a critical analysis, *Can. J. Phys.* **58**, 1200 (1980).
- ¹⁵ J. Kudrnovský and V. Drchal, Electronic structure of random alloys by the linear band-structure methods, *Phys. Rev. B* **41**, 7515 (1990).
 - ¹⁶ I. Turek, J. Kudrnovský, and V. Drchal, Nonlocal torque operators in *ab initio* theory of Gilbert damping in random ferromagnetic alloys, *Phys. Rev. B* **92**, 214407 (2015).
 - ¹⁷ A. A. Starikov, P. J. Kelly, A. Brataas, Y. Tserkovnyak, and G. E. W. Bauer, Unified First-Principles Study of Gilbert Damping, Spin-Flip Diffusion, and Resistivity in Transition Metal Alloys, *Phys. Rev. Lett.* **105**, 236601 (2010).
 - ¹⁸ A. Sakuma, First-Principles Study on the Gilbert Damping Constants of Transition Metal Alloys, Fe-Ni and Fe-Pt Systems, *J. Phys. Soc. Jpn.* **81**, 084701 (2012).
 - ¹⁹ S. Mankovsky, D. Ködderitzsch, G. Woltersdorf, and H. Ebert, First principles calculation of the Gilbert damping parameter via the linear response formalism with application to magnetic transition metals and alloys, *Phys. Rev. B* **87**, 014430 (2013).
 - ²⁰ I. Turek, J. Kudrnovský, and V. Drchal, Ab initio theory of galvanomagnetic phenomena in ferromagnetic metals and disordered alloys, *Phys. Rev. B* **86**, 014405 (2012).
 - ²¹ S. Huang, W. Li, X. Li, S. Schönecker, L. Bergqvist, E. Holmström, L. K. Varga, L. Vitos, Mechanism of magnetic transition in FeCrCoNi-based high-entropy alloys, *Mater. Des.* **103**, 71-74 (2016).
 - ²² H. Akai, P. H. Dederichs, Local moment disorder in ferromagnetic alloys, *Phys. Rev. B* **47**, 8739 (1993).
 - ²³ See Fig. 17 in Ref.2.
 - ²⁴ H. Ebert, S. Mankovsky, K. Chadova, S. Polesya, J. Minar, and D. Ködderitzsch, Calculating linear-response functions for finite temperatures on the basis of the alloy analogy model, *Phys. Rev. B* **91**, 165132 (2015).
 - ²⁵ G. D. Samolyuk, S. Mu, A. F. May, B. C. Sales, S. Wimmer, S. Mankovsky, H. Ebert, and G. M. Stocks, Temperature dependent electronic transport in concentrated solid solutions of the 3d-transition metals Ni, Fe, Co and Cr from first principles, *Phys. Rev. B* **98**, 165141 (2018).
 - ²⁶ M. C. Cadevillet, V. Pierron-Bohnest, J. M. Sanchez, Modelling of the electrical resistivity of ferromagnetic and paramagnetic intermetallic compounds, *J. Phys: Condens. Matter* **4** 9053-9066 (1992), (Fig.3 there).
 - ²⁷ R. H. Brown, P. B. Allen, D. M. Nicholson, W. H. Butler, Resistivity of Strong-Scattering Alloys: Absence of Localization and Success of Coherent-Potential Approximation Confirmed by Exact Supercell Calculations in $V_{1-x}Al_x$, *Phys. Rev. Lett.* **62**, 661 (1989).
 - ²⁸ P. Singh, A. V. Smirnov, and D. D. Johnson, Atomic short-range order and incipient long-range order in high-entropy alloys, *Phys. Rev. B* **91**, 224204 (2015).
 - ²⁹ D. Wagenknecht, L. Šmejkal, Z. Kašpar, J. Sinova, T. Jungwirth, J. Kudrnovský, K. Carva, I. Turek, Temperature-dependent resistivity and anomalous Hall effect in NiMnSb from first principles, *Phys. Rev. B* **99**, 174433 (2019).
 - ³⁰ A. J. Pindor, J. Staunton, G. M. Stocks, H. Winter, Disordered local moment state of magnetic transition metals: a self-consistent KKR CPA calculation, *J. Phys. F: Met. Phys.* **13**, 979-989 (1983).
 - ³¹ J. Kudrnovský, V. Drchal, I. Turek, S. Khmelevskiy, J. K. Glasbrenner, and K. D. Belashchenko, Spin-disorder resistivity of ferromagnetic metals: the disordered local moment approach, *Phys. Rev. B* **86**, 144423 (2012).
 - ³² V. Drchal, J. Kudrnovský, D. Wagenknecht, I. Turek, Spin-disorder resistivity of random fcc-NiFe alloys, *Phys. Rev. B* **98**, 134442 (2018).
 - ³³ S. Khmelevskiy, K. Palotás, L. Szunyogh, and P. Weinberger, Ab initio calculations of the anisotropic magnetoresistance in $Ni_{1-c}Fe_c$ bulk alloys, *Phys. Rev. B* **68**, 012402 (2003).